Saline Hybrid Nanomaterials with Phthalocyanine and Tetraphenylporphine Anions Showing Efficient Singlet-O$_2$ Production and Photocatalysis

– SUPPORTING INFORMATION –

Marieke Poß and Claus Feldmann*

Institute of Inorganic Chemistry

Karlsruhe Institute of Technology (KIT)

Engesserstraße 15, 76131 Karlsruhe (Germany)

Fax: (+49) 721-6084892

E-mail: claus.feldmann@kit.edu

Content

1. Analytical Tools

Scanning electron microscopy (SEM) was carried out with a Zeiss Supra 40 VP microscope (Germany). Diluted aqueous suspensions of the as-prepared $Gd_4^{3+}[AlPCS_4]_3^{4-}$ and $La_4^{3+}[TPPS_4]_3^{4-}$ IOH-NPs were deposited on silicon wafers and thereafter dried by evaporation. The acceleration voltage was at 1-2 kV to avoid charging of the samples; the working distance was 3 mm.

Dynamic light scattering (DLS) of $Gd_4^{3+}[AlPCS_4]_3^{4-}$ and $La_4^{3+}[TPPS_4]_3^{4-}$ IOH-NPs was conducted with aqueous suspensions (1 mg of IOH-NPs per ml of water) in polystyrene cuvettes applying a Nanosizer ZS from Malvern Instruments (U.K.) that was equipped with a laser with an emission wavelength of 633 nm.

Fourier-transformed infrared (FTIR) spectra were recorded on a Bruker Vertex 70 FT-IR spectrometer (Bruker, Germany) in the range of 4000 to 370 cm^{-1} with a resolution of 4 cm^{-1}. For sample preparation, 1 mg of dried IOH-NP sample was pestled with 300 mg of dried KBr and pressed to a pellet. All measurements were recorded in transmission geometry.

Differential thermal analysis (DTA) and thermogravimetry (TG) were performed with a STA409C device (Netzsch, Germany). The measurements were performed in air to guarantee for complete combustion of the organic anions. Prior to measurement, all samples were dried in vacuum to remove all volatiles (especially water). 20 mg of $Gd_4^{3+}[AlPCS_4]_3^{4-}$ or $La_4^{3+}[TPPS_4]_3^{4-}$ were filled in corundum crucibles and thereafter heated to 1000 °C with a heating rate of 1 K/min.

Elemental analysis (C/H/N/S analysis) of $Gd_4^{3+}[AlPCS_4]_3^{4-}$ and $La_4^{3+}[TPPS_4]_3^{4-}$ IOH-NPs were performed via thermal combustion with an Elementar Vario Microcube device (Elementar, Germany) at a temperature of about 1100 °C. Prior to analysis, the samples were dried in vacuum to remove all volatiles (especially water)

Ultraviolett/visible (UV/Vis) spectra were recorded with a Cary Scan 100 (Varian, Germany). Aqueous suspensions of $Gd_4^{3+}[AlPCS_4]_3^{4-}$ and $La_4^{3+}[TPPS_4]_3^{4-}$ IOH-NPs as well as aqueous solutions of $H_4(AlPCS_4)$ and $H_4(TPPS_4)$ as references were measured against pure water in quartz glass cuvettes (quality grade 6Q, Starna, Germany).

2. Synthesis of IOH NPs

$Gd_4{}^{3+}[AlPCS_4]_3{}^{4-}$ *IOH-NPs:* $H_4(AlPCS_4)$ (23 mg, 0.025 mmol, Frontier Scientific, U.S.A.) was dissolved in water (30 mL). This solution was heated to 55 °C and stirred vigorously. Thereafter, an aqueous solution (0.5 mL) containing $GdCl_3 \times 6H_2O$ (28 mg, 0.075 mmol, 99%, Aldrich, Germany) were injected. After 2 min of intense stirring, the nanoparticles were separated via centrifugation (25,000 rpm, 15 min). To remove all remaining salts, the dark blue $Gd_4{}^{3+}[AlPCS_4]_3{}^{4-}$ IOH-NPs were resuspended in and centrifuged from H_2O three times. Thereafter, the as-prepared $Gd_4{}^{3+}[AlPCS_4]_3{}^{4-}$ IOH-NPs can be resuspended in H_2O, HEPES buffer or Dextran solution via mechanic stirring or ultrasonification in order to obtain colloidally stable suspensions with a weight content of 1 to 10 mg/mL. To prevent untimely $^1O_2$ production, the IOH-NPs were protected from light during synthesis, purification, and storage.

$La_4{}^{3+}[TPPS_4]_3{}^{4-}$ *IOH-NPs:* $H_4(TPPS_4)$ (20 mg, 0.016 mmol, Frontier Scientific, U.S.A.) was dissolved in water (30 mL). This solution was stirred vigorously. Thereafter, an aqueous solution (0.5 mL) containing $LaCl_3 \times 7H_2O$ (62 mg, 0.166 mmol, 99%, Aldrich, Germany) were injected. After 2 min of intense stirring, the nanoparticles were separated via centrifugation (25,000 rpm, 15 min). To remove all remaining salts, the dark blue $La_4{}^{3+}[TPPS_4]_3{}^{4-}$ IOH-NPs were resuspended in and centrifuged from H_2O three times. Thereafter, the as-prepared $La_4{}^{3+}[TPPS_4]_3{}^{4-}$ IOH-NPs can be resuspended in H_2O, HEPES buffer or Dextran solution via mechanic stirring or ultrasonification in order to obtain colloidally stable suspensions with a weight content of 1 to 10 mg/mL. To prevent untimely $^1O_2$ production, the IOH-NPs were protected from light during synthesis, purification, and storage.

3. Material Characterization

3.1 Electron Microscopy (SEM)

The particle diameter of the as-prepared $Gd_4{}^{3+}[AlPCS_4]_3{}^{4-}$ and $La_4{}^{3+}[TPPS_4]_3{}^{4-}$ IOH-NPs was investigated via scanning electron microscopy (SEM). For both types of IOH-NPs, the mean particle diameter was determined by statistical evaluation of at least 100 nanoparticles from SEM overview images. Since the resolution of the applied SEM device was at 1.6 nm, transmission electron microscopy (TEM) was not performed and not required to investigate the particle size and shape. Moreover, it needs to be considered that the high acceleration voltage of a TEM (i.e. 200-300 keV) causes a much faster degradation of the IOH-NPs than a SEM with significantly lower electron energy (acceleration voltage of 1 to 20 keV).

Figure S1 shows SEM overview images of the as-prepared $Gd_4{}^{3+}[AlPCS_4]_3{}^{4-}$ and $La_4{}^{3+}[TPPS_4]_3{}^{4-}$ IOH-NPs. Both look very comparable which is to be expected in view of similar conditions of synthesis and the comparable composition of the IOH-NPs.
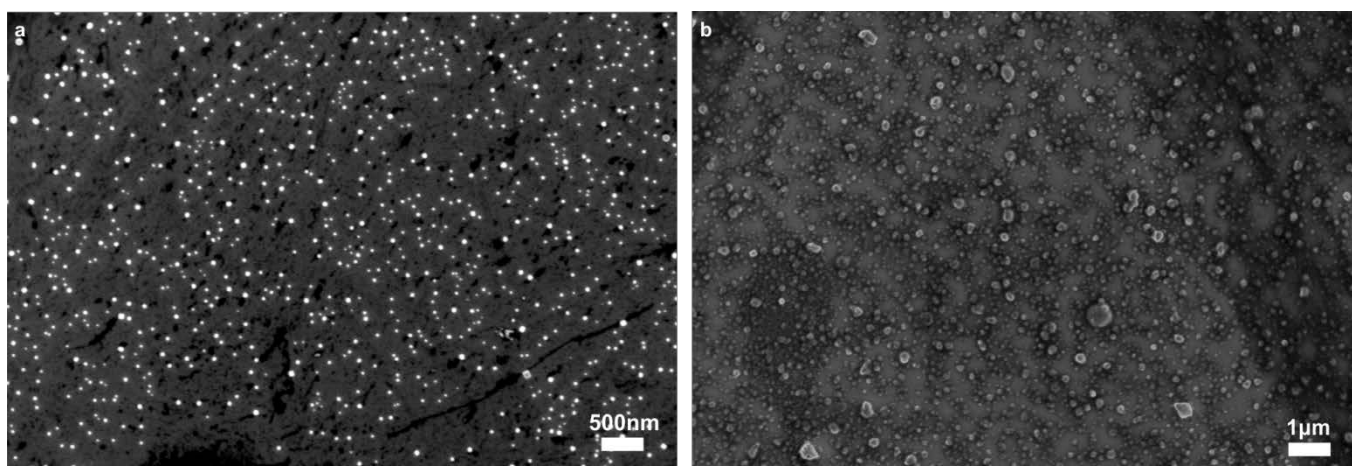
Figure S1. SEM images of the as-prepared $Gd_4^{3+}[AlPCS_4]_3^{4-}$ (left) and $La_4^{3+}[TPPS_4]_3^{4-}$ (right) IOH-NPs.

3.2 Dynamic Light Scattering (DLS)

Particle diameter and size distribution of the as-prepared $La_4^{3+}[TPPS_4]_3^{4-}$ IOH-NPs were also validated via DLS in water. As a result a mean hydrodynamic diameter of 68(10) nm was determined (Figure S2). This value is larger in comparison to the mean diameter obtained from electron microscopy since it reflects the hydrodynamic diameter and the presence of a rigid layer of adsorbed solvent molecules on the particle surface. The DLS analysis should not be overestimated due to the fact that the IOH-NPs are currently not stabilized by any specific surface-active agent (e.g., dextran, protamine, polyethylene glycol). Therefore, certain agglomeration in water (as a highly polar solvent with very high surface tension) is to be expected.

Finally, it is to be noted that the hydrodynamic diameter of the $Gd_4^{3+}[AlPCS_4]_3^{4-}$ IOH-NPs could not be detected by DLS since the laser ($\lambda = 633$ nm) results in an excitation of the nanoparticles. The resulting fluorescence of the $Gd_4^{3+}[AlPCS_4]_3^{4-}$ IOH-NPs, however, superimposes and falsifies the scattered light required for DLS analysis.
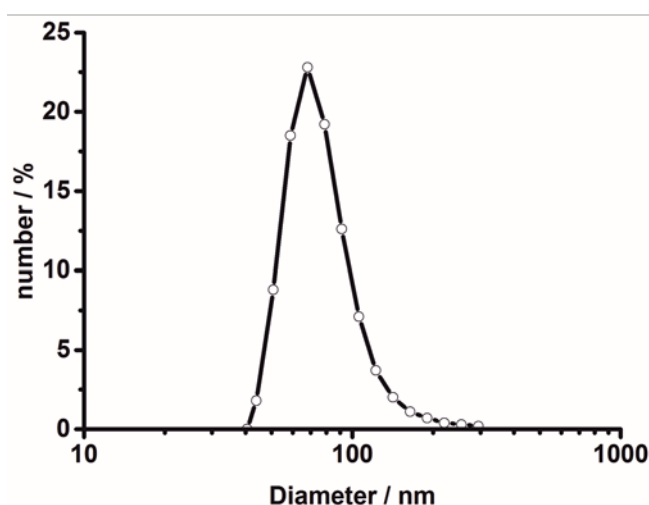

Figure S2. Size distribution of $La_4^{3+}[TPPS_4]_3^{4-}$ IOH-NPs in water according to DLS.

3.3 Infrared Spectroscopy (FT-IR)

To verify the chemical composition qualitatively and to especially prove the presence of the respective anion of the $Gd_4^{3+}[AlPCS_4]_3^{4-}$ and $La_4^{3+}[TPPS_4]_3^{4-}$ IOH-NPs, FT-IR was involved (Figure S3). The comparison of spectra of $Gd_4^{3+}[AlPCS_4]_3^{4-}$ IOH-NPs with the starting material $H_4(AlPCS_4)$ are very comparable and show all characteristic vibrations of aluminium(III) chlorido phthalocyanine tetrasulfonate, including $v(N–H)$: 3500-3330 cm^{-1}, $v(C=N)$: 1660-1480 cm^{-1}, $v_{as}(SO_3)$: 1600-1300 cm^{-1}, $v_s(SO_3)$: 1250-950 cm^{-1} (Figure S3). Moreover, $v(O−H)$ at 3600-3200 cm^{-1} indicates the presence of H_2O. Similarly, the comparison of the $La_4^{3+}[TPPS_4]_3^{4-}$ IOH-NPs with $H_4(TPPS_4)$ as a reference shows all characteristic vibrations of tetraphenylporphine sulfonate, including $v(N–H)$: 3500-3330 cm^{-1}, $v(C=C)$: 1600-1500 cm^{-1}, $v_{as}(SO_3)$: 1600-1300 cm^{-1}, $v_s(SO_3)$: 1250-950 cm^{-1} (Figure S3b). Again, $v(O−H)$ at 3600-3200 cm^{-1} indicates the presence of H_2O. It is to be noted that a certain broadening of all vibrations of the IOH-NPs is related to the non-crystallinity of the nanoparticles.
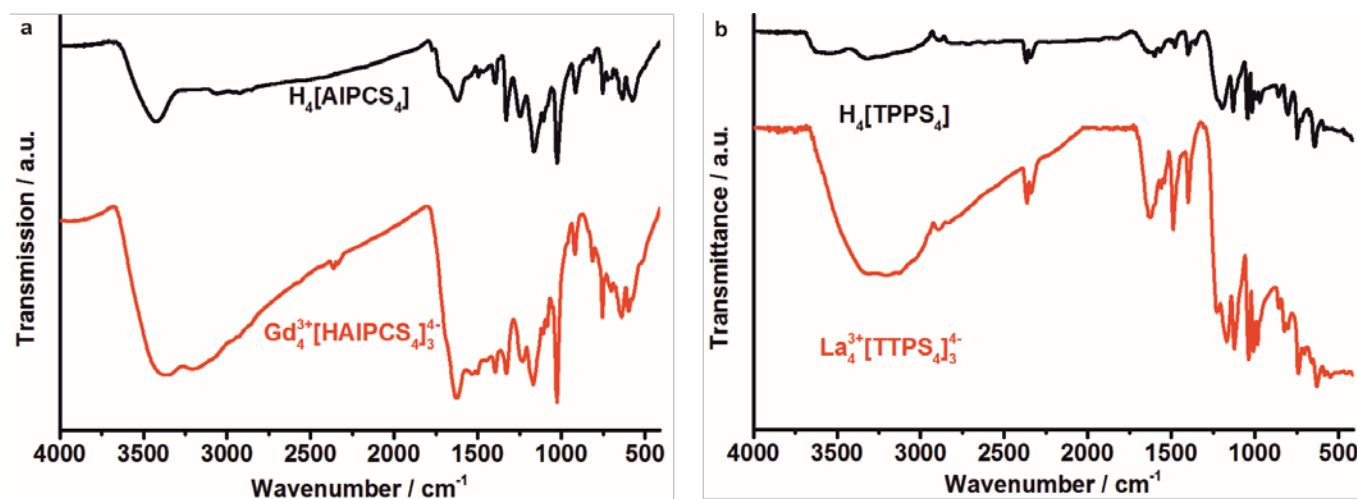

Figure S3. FT-IR spectra of the as-prepared $Gd_4^{3+}[AlPCS_4]_3^{4-}$ (left) and $La_4^{3+}[TPPS_4]_3^{4-}$ (right) IOH-NPs with the spectra of the relevant starting materials $H_4(AlPCS_4)$ and $H_4(TPPS_4)$ as references.

3.4 Thermogravimetry (TG)

To quantify the chemical composition and the cation-to-anion ratio in the $Gd_4^{3+}[AlPCS_4]_3^{4-}$ and $La_4^{3+}[TPPS_4]_3^{4-}$ IOH-NPs, TG was performed to study the total combustion of the organic anion. To this concern, $Gd_4^{3+}[AlPCS_4]_3^{4-}$ shows five-step decomposition in air and in a temperature range of 30-1000 °C with a total weight loss of 84.8% (Figure S4a). Hereof, the first step (20-200 °C, 4.4%) can be attributed to surface-adhered water on the amorphous IOH-NPs. The dominating weight loss up to 1000 °C (80.4%) relates to the thermal decomposition of the organic anion. This value corresponds well to the calculated weight loss of 80.5% for the assumed composition $Gd_4^{3+}[AlPCS_4]_3^{4-}$. The thermal remnant of the TG analysis was identified via X-ray powder diffraction (XRD) as a mixture of $(GdO)_2SO_4$, Gd_2O_3 and $Gd_3Al_5O_{12}$.

$La_4^{3+}[TPPS_4]_3^{4-}$ shows a four-step decomposition in a temperature range of 30-1000 °C in air with a total weight loss of 84.6% (Figure S4b). Hereof, the first step (20-200 °C, 3.2%) can be attributed to surface-adhered water on the amorphous IOH-NPs. The dominating weight loss up to 1000 °C (81.4%), moreover, again relates to the combustion of the organic anion. This value also correspond well to the calculated weight loss of 84.0% for the assumed composition $La_4^{3+}[TPPS_4]_3^{4-}$. Finally, the thermal remnant of the TG analysis was identified via XRD as $(LaO)_2SO_4$.
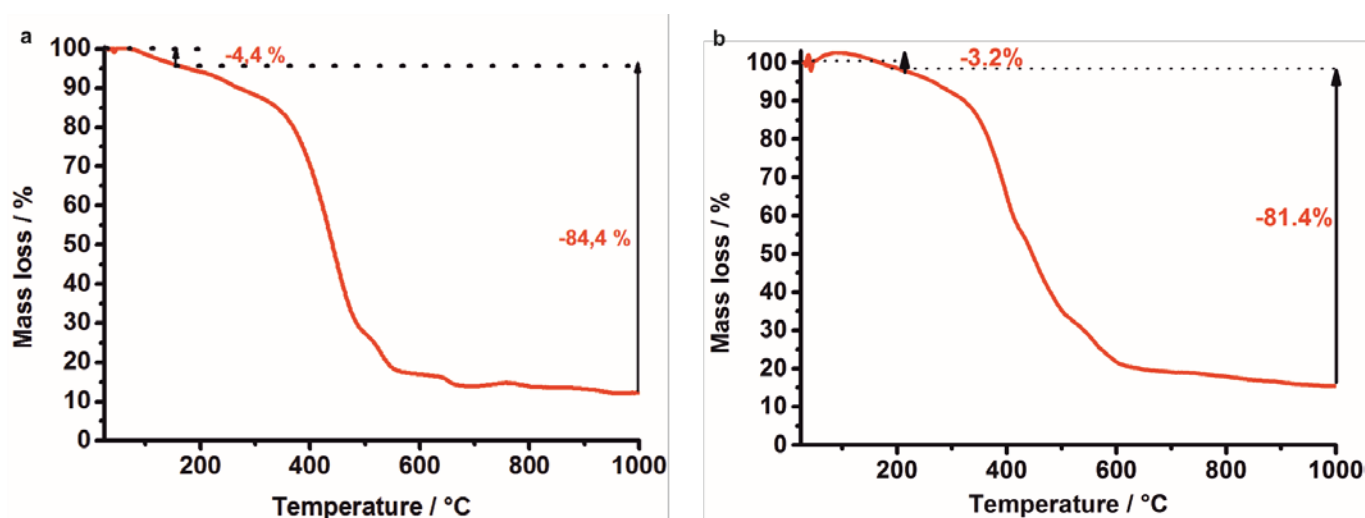

Figure S4. TG analysis of the $Gd_4^{3+}[AlPCS_4]_3^{4-}$ (left) and $La_4^{3+}[TPPS_4]_3^{4-}$ (right) IOH-NPs. The measurements were performed in air with a total sample weight of 20 mg and with a heating rate of 1 K/min.

The chemical composition and the cation-to-anion ratio of the $Gd_4^{3+}[AlPCS_4]_3^{4-}$ and $La_4^{3+}[TPPS_4]_3^{4-}$ IOH-NPs was confirmed by elemental analysis that shows good agreement between the measured data and the calculated data for the C, H, N, and S content (*see main paper*).
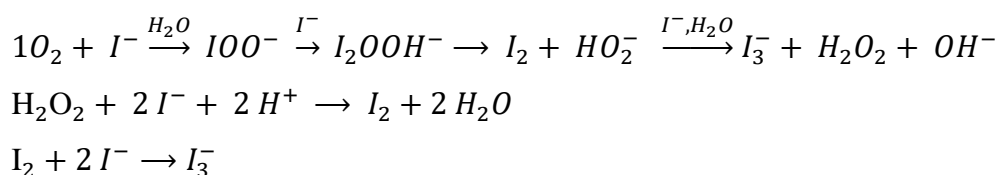
Taking all analytical data together (FT-IR, EDX, TG, EA), the composition of the $Gd_4^{3+}[AlPCS_4]_3^{4-}$ and $La_4^{3+}[TPPS_4]_3^{4-}$ IOH-NPs is reliably substantiated.

4. Determination of the Quantum Yield for Singlet Oxygen Production

The *singlet oxygen quantum yield (φ_Δ) of the $Gd_4^{3+}[AlPCS_4]_3^{4-}$ IOH-NPs* was determined by a relative method using DPBF (1,3-diphenylisobenzofuran) as chemical quencher for singlet oxygen.[1] Thus, φ_Δ is proportional to the disappearance of the DBPF absorption band in the UV-Vis spectra. To perform the respective experiments, DPBF was first dissolved in DMF to obtain the corresponding solution (100 μM), which was formulated with Kolliphor EL and then diluted with O_2-saturated, deionized water to 50 mL (in sum containing 0.2 % of DMF and 0.1 % of Kolliphor EL). The DPBF solution (2 mL) was then mixed with the $Gd_4^{3+}[AlPCS_4]_3^{4-}$ IOH-NP suspension in H_2O (8 μM, 2 mL) in the dark to obtain a mixture of

DPBF and the IOH-NPs (in sum containing 50 μM of DPBF, 4 μM of $Gd_4^{3+}[AlPCS_4]_3^{4-}$, 0.1 % of DMF, and 0.05 % of Kolliphor EL). This mixture was irradiated with red light immediately. The DPBF degradation was monitored at 413 nm along with irradiation time.[1] The singlet oxygen quantum yield (φ_Δ) was calculated by the equation: $\Phi_\Delta = \Phi_\Delta^{Std} \frac{I^{Std} R}{I R^{Std}}$; where φ_Δ^{Std} is the singlet oxygen quantum yield for the standard in H_2O ($\varphi_\Delta = 0.34$);[2] R and R^{Std} are the DPBF photobleaching rates in the presence of the IOH-NP sample and the standard, respectively. They were calculated by the equation: $\ln(A_0/A_t) = R\,t$, where t, A_0, A_t are the irradiation time, the absorbance at $t = 0$, and the absorbance at the time of measurement, respectively. I and I^{Std} are the absorbance at the position of the Q band (area under the absorption spectra in the 610-800 nm range) of sample and standard, respectively. As the light source a 1000 W Xe-lamp equipped with a solar filter (LOT Quantum Design, Germany) and a 610 nm edge filter (Schott, Germany) were used.

The *singlet oxygen quantum yield (φ_Δ) of the $La_4^{3+}[TPPS_4]_3^{4-}$ IOH-NPs* was determined by the iodide method, based on the reaction of $^1O_2$ (produced by the photodynamic reaction) with I^- in the presence of $(NH_4)_2MoO_4$ as a catalyst.[3] The amount of I_3^- produced in the reaction is directly proportional to the concentration of generated $^1O_2$:

$$1O_2 + I^- \xrightarrow{H_2O} IOO^- \xrightarrow{I^-} I_2OOH^- \longrightarrow I_2 + HO_2^- \xrightarrow{I^-,H_2O} I_3^- + H_2O_2 + OH^-$$

$$H_2O_2 + 2\,I^- + 2\,H^+ \longrightarrow I_2 + 2\,H_2O$$

$$I_2 + 2\,I^- \longrightarrow I_3^-$$

The iodide method was chosen instead of the above described DPBF method due to the fact that the absorption of TPPS at 417 nm is too close to the absorption of DBPF at 413 nm. As a consequence, the evaluation of the singlet oxygen quantum yield is not possible.

For the experiments, 0.1 M of KI, 10 μM of $(NH_4)_2MoO_4$ in 0.02 M of sodium-potassium phosphate buffer at pH 6.2 were used. 2 mL of water containing different concentrations of the $La_4^{3+}[TPPS_4]_3^{4-}$ IOH-NPs were mixed in 2 mL of the detection reagent so that the absorbance at 413 nm did not exceed the value 0.1 to avoid the shielding effect. These mixtures were irradiated with a 1000 W Xe-lamp equipped with a solar filter emulating daylight of (LOT Quantum Design, Germany). The formation of I_3^- was monitored at 351 nm along with irradiation time.

The following relationship can be derived from the theory of the photooxidation of the substrate (here I^-) by $\Phi_\Delta = \frac{r_{ox}}{I_a} \frac{f_D k_r [I^-]}{k_d + k_q[I^-]} = f_D p$, where φ_Δ is the quantum yield of oxidation of I^-; r_{ox} is the rate of oxidation of I^-; I_a is the intensity of light absorbed by the irradiated suspension; k_r is the bimolecular rate constant of the chemical reaction of I^- with $^1O_2$; k_a is the rate constant of quenching of $^1O_2$ by the solvent; k_q is the overall bimolecular rate constant of $^1O_2$ quenching by I^-; f_D is the quantum yield of $^1O_2$; and p is the fraction of $^1O_2$ chemically reacting with I^-. With conditions of constant source output and given photosensitizer

absorbance at 413 nm, the change of the absorbance of the triiodide band ($A(I_3^-)$) in time is proportional to the rate of oxidation of I^- (φ_Δ). In direct relation to the Beer-Lambert law, the expression $1- 10^{-A}$ (where A is the absorbance of the photosensitizer at 413 nm) is directly proportional to the fraction of the radiation absorbed by the photosensitizer. The slope B of the plot of the absorbance of the I_3^- band at 351 nm against the irradiation time is proportional to the rate of oxidation of I^- or of the formation of the resulting I_3^-. The slope of the dependence of slope B on the expression $1\text{-}10^{-A}$, denoted as k, is then directly proportional to the relative quantum yield φ_Δ of the oxidation, and thus, also to f_D.[3]

$^1O_2$ Quantum xield: As discussed above, the DPBF method[1,2] was used to determine the $^1O_2$ quantum yield of the $Gd_4^{3+}[AlPCS_4]_3^{4-}$ IOH-NPs. To this concern, the decrease of the DPBF absorption was monitored by optical spectra (*see main text: Figure 2a*). During irradiation no photodegradation of the phthalocyanine was observed, which is validated by the fact that no decrease of the Q band vibration as well as no formation of new absorption bands were observed. The photobleaching rate (R) of the IOH-NPs, which was calculated by the equation $\ln(A_0/A_t) = R\,t$ (see above), is depicted in Figure S5a.

For the determination of the $^1O_2$ quantum yield of the $La_4^{3+}[TPPS_4]_3^{4-}$ IOH-NPs, the Iodide method[3] was used as described above. Therefore, the absorbance of the pure photosensitizer $H_4(TPPS_4)$ was adjusted at 417 nm to a value less or equal than 0.1. A regression straight line was fitted through the experimental point for each absorbance. The slope *B*, its standard deviation and the correlation coefficient R were calculated for each of these straight lines (Figure S5b). The slope B was obtained from experimental data in the linear section of the plot of the increase in I_3^- absorbance versus the irradiation time, so that the correlation coefficient R of the linear regression was greater than 0.995. The determined slope of the increase in I_3^- absorbance was then plotted in a graph against $1\text{-}10^{-A}$, and the resulting values were again fitted by a straight line using a linear regression (Figure S5c). Again, the correlation function starts in the origin of the coordinate system. The slope of the dependence of *B* on $1\text{-}10^{-A}$– denoted as k – is directly proportional to the relative quantum yield of the singlet-oxygen production. By correlation of the quantum yield of $H_4(TPPS_4)$ solutions as given in the literature (i.e., 0.51 in aqueous solution) to the calculated slope k for $H_4(TPPS_4)$, one obtains the values of the quantum yield for the test substance by direct proportionality.[3]
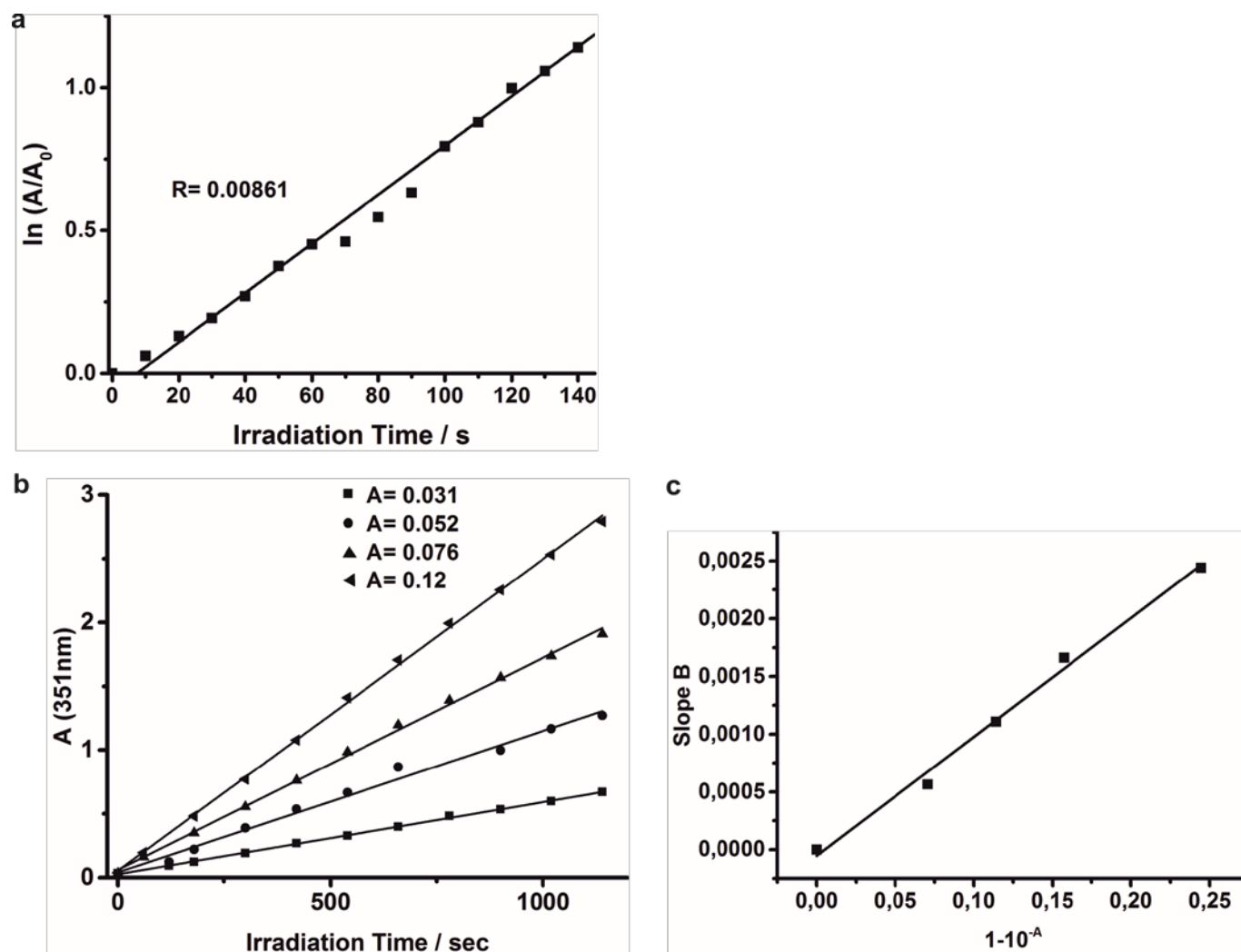
Figure S5. a) First-order plots for the degradation of DPBF by $^1O_2$ produced upon illumination of the $Gd_4^{3+}[AlPCS_4]_3^{4-}$ IOH-NPs. The slope of the plot corresponds to the photobleaching rate R. b) Dependence of the absorbance of the triiodide band on the radiation time for various concentrations of $H_4(TPPS_4)$ solutions in iodide reagent. A is the absorbance of $H_4(TPPS_4)$ at 417 nm. c) Relationship between the Slope B and the fraction of light $(1\text{-}10^{-A})$ absorbed by the photosensitizer for variously concentrated suspensions of $H_4(TPPS_4)$ in iodide reagent.

5. Dye-Degradation Studies

The photocatalytic activity was evaluated by the oxidative decomposition of Eriochrome Black T (EBT) as a model compound under simulated daylight using a Schott KL1500 LCD halogen cold light source equipped with a Philips Fibre Optic Lamp 6423FO (15 V, 150 W). The lamp can be equipped with a red glass filter to generate red light. Eriochrome Black T was chosen since its absorption band is outside the region of absorption by the photocatalysts. Thus, any significant photocatalytic decomposition of the dye by self-absorption can be excluded.

The degradation rate of the EBT dye was monitored by recording the variation of the absorption-band maximum at $\lambda_{max} = 516$ nm in the absorbance spectrum using a Varian Cary 100 spectrometer. In addition to the as-prepared $Gd_4^{3+}[AlPCS_4]_3^{4-}$ and $La_4^{3+}[TPPS_4]_3^{4-}$ IOH-NPs, the commercial photocatalyst Degussa P25 (80% anatase, 20% rutile, particle diameter: 25-30 nm with strong agglomeration) and the as-prepared blue-light-activated photocatalyst β-SnWO$_4$[4] were tested and compared in view of their performance. All measurements were performed with identical conditions, especially, using an equivalent absorbance of all photocatalysts ($A = 2.0$). To this concern, 8 µmol of $Gd_4^{3+}[AlPCS_4]_3^{4-}$, 8 µmol of $La_4^{3+}[TPPS_4]_3^{4-}$, 900 µM of anatase-TiO$_2$, and 160 µM of β-SnWO$_4$ were applied. All suspensions (20 mL, c(EBT) = 0.03 µmol/L) were placed in a beaker, continuously stirred magnetically and illuminated in intervals of 10 minutes. After each 10 minutes, 4 mL of the relevant suspension were filled into a 6Q quartz glass cuvette (Starna, Germany). The absorbance was determined via UV-Vis spectroscopy (Figure S6). Thereafter, analysed sample was re-added to the main suspension and the next 10-minutes interval of illumination was started.
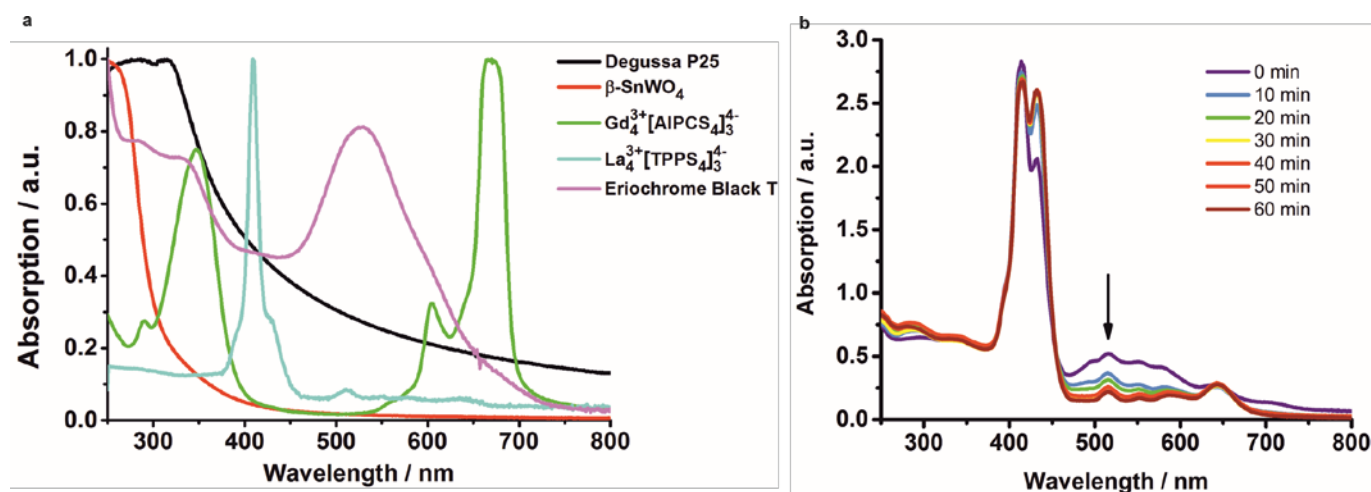

Figure S6. a) UV-Vis spectra of the $Gd_4^{3+}[AlPCS_4]_3^{4-}$ and $La_4^{3+}[TPPS_4]_3^{4-}$ IOH-NPs and the reference photocatalysts (Degussa P25, β-SnWO$_4$) as well as of pure Eriochrome Black T (EBT); b) Decrease of the EBT absorption band at 528 nm due to reaction of the dye with $^1O_2$ produced by $La_4^{3+}[TPPS_4]_3^{4-}$ IOH-NPs at different times of irradiation.

References

1. X.-S. Li, M.-R. Ke, W. Huang, C.-H. Ye and J.-D. Huang, *Chem. Eur. J.*, 2015, **21**, 3310.
2. J. Mosinger and Z. Miĉka, *J. Photochem. Photobiol. A,* 1997, **107**, 77.
3. W. P. Helman and A. B. Ross, *J. Phys. Chem. Ref. Data,* 1993, **22***,* 113.
4. J. Ungelenk and C. Feldmann, *Chem. Commun.*, 2012, **48**, 7838.
5. J. Ungelenk and C. Feldmann, *Appl. Catal. B*, 2012, **127**, 11.